6ICEGE 6th International Conference on Earthquake Geotechnical Engineering
1-4 November 2015
Christchurch. New Zealand

A Numerical Study of the Pressurized Gas Pipeline-Normal Fault Interaction Problem

A.G. Özcebe[1], R. Paolucci[2], S. Mariani[3], D. Santoro[4]

ABSTRACT

This paper explores the seismic response of continuous, pressurized gas-transmitting steel pipes subjected to normal fault rupture, through a series of parametric 3D finite element analyses. The constitutive and geometrical models are first verified through comparison with previously published centrifuge results covering the rupture propagation of a normal fault (Bransby et al., 2008), and with simple analytical calculations based on the theory of thin walled pressurized cylinders and metal plasticity with Mises yield criterion. The impact of different features of the buried pipeline-normal fault rupture interaction problem, like operating temperature and operating pressure, is then investigated by means of a practical example problem, with pre-selected geometry and material properties, according to the performance-based approach.

Introduction

In seismic design of pipelines, crossing of active faults has been recognized as one of the most challenging and project-affecting issues. Recent evidences in Kocaeli (1999) and L'Aquila (2009) earthquakes have confirmed that an unsafe design may result in undesired brittle pipeline failures (Eidinger et al., 2002; Paolucci et al., 2010), which may eventually lead to significant investment losses and social discomfort for the local communities. Seismic design of pipelines under fault crossing conditions is a complex fault-soil-pipeline interaction problem, which requires the account of soil and structural behaviour in nonlinear regime in typically 3D configurations. Existent analytical models developed for this purpose date back to the contribution by Newmark and Hall (1975) and its update by Kennedy et al. (1977), in which also the flexural behaviour of the pipeline was considered. After Kennedy et al. (1977), there has been a series of successful attempts on analytical modeling which are originally based on this work (Wang and Yeh, 1985; Karamitros et al., 2007, 2011; Trifonov and Cherniy, 2010, 2012).

Recently, Paolucci et al. (2010) have proposed an analytical model for strike-slip fault crossings based on the minimization of energy principle. The methodology of Paolucci et al. (2010) is presently being extended to normal fault crossings by also taking temperature and pressure differences into consideration.

[1]Dr., Department of Civil and Environmental Engineering (DICA), Politecnico di Milano, Post-Doctoral Research Associate, Milano, Italy, aliguney.ozcebe@polimi.it
[2]Prof., DICA, Politecnico di Milano, Milano, Italy, roberto.paolucci@polimi.it
[3]Prof., DICA, Politecnico di Milano, Milano, Italy, stefano.mariani@polimi.it
[4]M.Sc., Politecnico di Torino and ENI S.p.A., Post-Graduate Student in Petroleum Engineering and Operations, Torino, Italy, dome.santoro89@gmail.com

Thanks to the increasing computing capabilities, during the last two decades finite element modeling of the complex soil-structure interaction problem has also become quite popular (see e.g. Paolucci et al., 2010; Vazouras et al., 2012; Xie et al., 2013; Trifonov, 2015) as a solution alternative and/or complementary to the analytical techniques, leading more accurate and case-specific results, provided that the model is well constructed. Although it is now widely used, authors think that a significant gap still exists in the present state of information, in which the analysts/engineers are expected to assemble all the necessary components together when carrying out a numerical solution to the seismic design of pipelines under fault crossing conditions. Considering that such procedure development may not be always trivial, this paper aims at putting the fundamental background information on soil and engineering mechanics, together with the one of numerical analysis in a rather compact framework. This is thought to eventually serve as a reference for the future analysts/engineers interested in this subject.

In this paper, we start with a validation of the numerical model, in terms of boundary conditions, element types, and constitutive models using previously published physical model tests (Bransby et al., 2008) and analytical estimations of elastic and post-elastic values of pipe longitudinal and hoop stresses based on metal plasticity and structural mechanics. After the verification stage, we move to the detailed explanation of the finite element model featuring the interaction between a normal fault and the pipeline. Finally, we present a performance based way of elaborating the results, by also considering ALA Guidelines (2001; 2005) and Eurocode 8 (CEN, 2006).

Verification of the Numerical Model

In this section we first introduce a finite element simulation of a previously published centrifuge test in which normal fault propagation inside a dry frictional soil has been modeled under free-field conditions (i.e. in the absence of any structure). Successful modeling of this problem will ensure the adequacy of the finite element formulation, mesh fineness, representativeness of the constitutive model selected for the soil material, and the correct modeling of boundary conditions. Following the centrifuge verification, we will pass to verify the structural counterpart of the spatial resolution and accuracy of the finite element model, through simple analytical solutions derived from the fundamentals of engineering mechanics.

Verification study 1

The centrifuge setup used by Bransby et al. (2008) is shown in Figure 1. Fault offset with dip angle of 60° has been represented in terms of imposed displacements at the model boundaries.

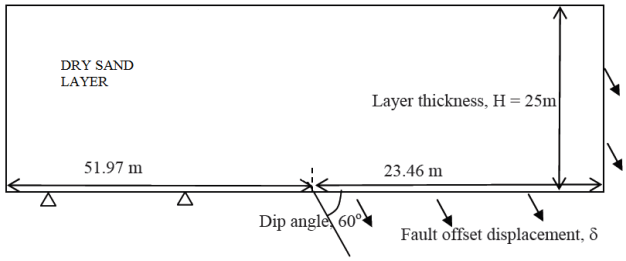

Figure 1: Physical model in prototype scale, scale factor =115 (after Bransby et al., 2008).

Dry soil layer, shown in Figure 1, is medium dense (D_r=60%), uniform silica sand, featuring an internal friction angle ϕ'=35° and a dilation angle ψ=6° (see Gaudin, 2002; Bransby et al., 2008).

The fault rupture has been simulated with Abaqus/Explicit (Dassault Systèmes, 2013), by smoothly increasing the boundary displacements to minimize the numerically induced propagation of spurious elastic waves inside the mesh. The dry sand layer has been modeled as an elastic-plastic material with Mohr-Coulomb yield function.

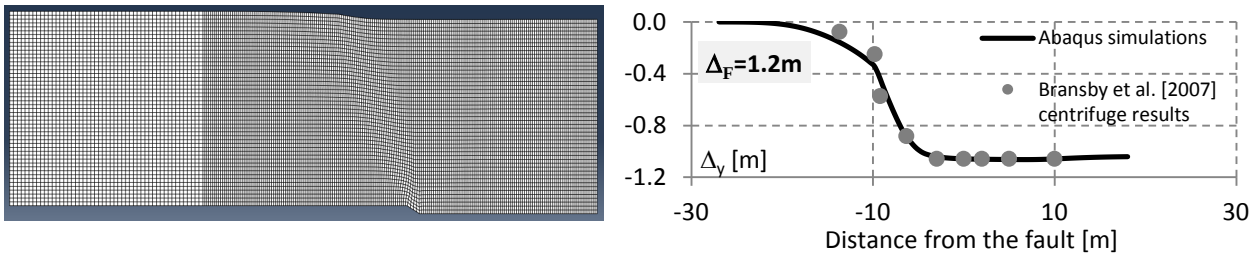

Figure 2: Deformed finite element mesh (left) and comparison of results for total fault offset of 1.2 m (right) (after Bransby et al., 2008).

Figure 2 shows the deformed mesh, and a comparison of numerical and experimental data in terms of vertical displacements measured at a depth of z= 0.9m at a specified fault offset, Δ_F=1.2 m. To model, with a sufficient degree of accuracy, the propagation of the fault in the dry sand up to the selected offset, a fine mesh has been adopted with characteristic element size of about 0.25 m. The graph in Figure 2 shows that the numerical predictions are in a good agreement with the centrifuge test outputs for the considerably large fault offset of 1.2 m, which can be considered as a representative value for a M_w=6.0-6.5 event. As a result of this verification study, accuracy of the model in terms of boundary conditions, finite strain kinematics, resolution of the spatial discretization, and constitutive modeling of continuum (i.e. soil) finite elements have been confirmed as satisfactory.

Verification study 2

A gas transmission pipeline has been considered, featuring average radius R_{av}= 601.6 mm and wall thickness t =18.9 mm, with a burial depth of H= 1.5m, measured from the top of its cross-section. The longitudinal and hoop stresses, induced by the operating conditions (internal pressure p=7.5 atm and temperature difference ΔT= 45°C), provided by the numerical model have been checked against the following analytical estimations in the ideal situation of no defects and homogeneous geometry along the pipe longitudinal axis. By disregarding the self weight and the confining pressure of the soil around the pipeline, due to the shallow burial, the circumferential stress is given by the Mariotte formula:

$$\sigma_\theta^p = {pR_{av}}/{t} \quad (1)$$

Equation (1) may be written by imposing the equilibrium on the longitudinal cross section of a pressurized thin-wall pipe, in which σ_θ^p is the pressure induced hoop stress (= 238.7 MPa). By

assuming now that the pipe is free to deform axially, the longitudinal strain (ε_l) can be obtained via:

$$\varepsilon_l = \frac{1}{E}\left(\sigma_l^p - \nu\sigma_\theta^p\right) \tag{2}$$

where the through the thickness stress term has been purposely disregarded. E and ν are the Young's modulus and Poisson's ratio of the pipe steel, respectively. Considering now the axial constraint (ε_l=0) on the pipe segment, pressure-induced longitudinal stress σ_l^p could be stated as: $\sigma_l^p = \nu\sigma_\theta^p$ (= 71.6 MPa).

Moving now to the effects of the temperature increase ΔT due to gas flow in the pipeline, the same plane-strain like condition considered before leads to a temperature-induced longitudinal stress, $\sigma_l^{\Delta T}$, provided by:

$$\sigma_l^{\Delta T} = -E\alpha_l\Delta T \tag{3}$$

where, α_l is the thermal expansion coefficient of the pipe steel (in 1/°C or 1/°K).

With a standard API steel, featuring E = 210 GPa, ν= 0.3, α_l= 1.3x10^{-5} 1/°C, for an internal pressure p = 7.5 atm and stationary temperature variation ΔT= 45°C, the longitudinal and hoop stress estimates are as gathered in Table 1, where a comparison is also reported with the outcomes of the finite element simulations. Here, two operating conditions are considered and the corresponding pipe longitudinal and hoop stresses are shown in terms of their total.

Table 1: Comparison of pipe stresses caused by the operating conditions.

Condition	**σ_l [MPa]**		**σ_θ [MPa]**	
	Analytical	***Numerical***	***Analytical***	***Numerical***
p=7.5 atm, ΔT=0°C	71.6	≈ 72.6	238.7	≈ 243
p=7.5 atm, ΔT=45°C	-51.3	≈ -51.3	238.7	≈ 243

Table 1 shows a noteworthy agreement between the numerical solutions and the relevant simplified theoretical estimations. The slight difference between the two sets of values mainly stems from having neglected the weight and the confining pressure induced by the soil in the analytical calculations, and from the approximation of the circular pipe cross-section with discrete quadrilateral elements in the numerical model.

Finally, by considering that the pipeline is shallowly buried and is quite stiff compared to the confining ground, it appears reasonable to assume no cross-sectional deformation (i.e. no ovalization), when the fault offsets. This condition allows setting to zero the shear stress components along the pipe wall, and yielding can be checked by computing the Mises stress according to Equation (4).

$$\sigma_M^2 = \frac{1}{2}[(\sigma_\theta - \sigma_l)^2 + \sigma_l^2 + \sigma_\theta^2] \quad (4)$$

where the through-the-thickness component has been once again disregarded. Once we impose σ_θ= 238.7 MPa, at yielding σ_M=σ_y=450 MPa we may find the two following values for the longitudinal stress: $\sigma_{yl,t}$=520 MPa for tensile states and $\sigma_{yl,c}$=-280 MPa for compressive states, respectively. A comparison with relevant numerical values shows once again a good match between the two approaches.

Numerical Modeling of the Normal Fault-Buried Pipeline Interaction

Having validated the finite element approach as far as the free-field (VS-1) and operational (VS-2) loading conditions are concerned, we move now to the numerical analysis of the soil-structure interaction problem when the normal fault offsets. In this section, we briefly discuss the main features of the adopted numerical models, in terms of model definition, analysis steps, and boundary conditions. Additional information is to be provided by the corresponding future journal paper.

Model definition

Allowing for the target geometry of the problem at hand, in the simulations, 8-node reduced integration brick elements with hourglass control (C3D8R or C3D8RT) have been selected to spatially discretize the soil. On the other hand, the moderately thin pipeline has been discretized with 4-node shell elements with reduced integration and hourglass control (S4R and S4RT). In accordance with the settings adopted in the verification examples, in the region close to the fault crossing, where the strongest nonlinearities are expected, spatial discretization has been enhanced through a properly fine mesh, in terms of both soil and structural elements. Away from that region, to reduce the computational burden, element densities have been progressively reduced. Considering the material properties, besides what already discussed in the previous section, it is worth mentioning that the dry sand has been modeled as elastic-plastic, with a Mohr-Coulomb yield surface, featuring ϕ'=35° and ψ=5°. The contact surface between pipe and soil has been modeled with so-called interface elements (or contact elements), having the friction coefficient equal to *tan* 0.67ϕ' representing the interaction between dry sand and the smooth steel surface. One may refer to ALA Guidelines (2001; 2005) for the relevant friction coefficients.

Analysis steps and boundary conditions

A two-stage loading process has been considered. In stage 1, the operating internal gas pressure (p=7.5 atm), temperature difference, (ΔT=45°C), and the gravity load are invoked in a quasi-static manner. In stage 2, boundary conditions corresponding to a smoothly increasing fault offset have been provided along the model boundaries (*with a non-constant rate to prevent numerical induced elastic waves, on average 2 meters of fault offset is provided in 4 seconds*), on the soil and pipe external surfaces as a kind of far-field condition. The relevant boundary conditions are sketched in Figure 3, where it is shown that pipe and soil surfaces on the footwall side (left hand side in the figure) are both fixed, while the hanging wall side is displaced as whole. One may also observe that the fault offset has been distributed within a band of 1 m. This

allows imposing a realistic condition as well as providing improved fault rupture propagation due to limited distortion of the elements across the footwall/hanging wall at the base of the numerical model.

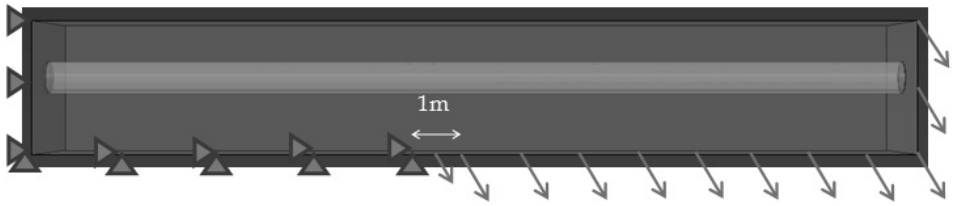

Figure 3: Numerical model (not to scale) showing the imposed displacement BC's.

To ensure a ductile response of the pipeline subjected to fault rupture, the physical anchor points, elbows and bents should be placed sufficiently far away from the expected fault crossing zone. To correctly represent the stress field along before any discontinuity occurs in the fault, the length of the pipe segment numerically modeled has to be appropriately set. Possible disturbances or numerical artifact showing up around the zone where the boundary conditions are imposed, and affecting the values of longitudinal stress values presented in Table 1, are to be kept away from the fault. Further, the modeled pipe segment must be sufficiently long to keep the fault induced axial strain as zero or negligible far away from the fault crossing. It has been observed that at any decreasing dip angle, the pipeline undergoes larger average axial strain induced by the fault movement, since the horizontal component of the fault motion increases. Accordingly, the longitudinal length is a function of anchor length (L_a) of the considered pipe segment, which can be approximated as:

$$L_a = \frac{EA\varepsilon_a}{\tau_u} \tag{5}$$

where; L_a is the anchor length; E is the Young's modulus of the pipe steel; A is the pipe cross-sectional area, ε_a is the fault induced axial strain; and τ_u is the interface friction acting on a 1-meter long pipe external surface. In order to determine the τ_u value, ALA Guidelines (2001; 2005) may be used.

Besides the dip angle, ε_a increases with increasing fault offset. Since burial depth has an important effect on τ_u, it also affects ε_a. By considering the parameters of burial depth ($Z=H+D/2\approx1.5+0.6=2.1$ m), the dip angle (dip= 70°-80°), and a total fault offset of maximum $\Delta_{\square}$= 2.0 m, we found out that total model length L_m= 2000 m becomes sufficient to keep the fault induced axial longitudinal stresses in the pipe to negligible values close to the boundaries.

Assessment of the Analysis Outcomes within a Performance Based Framework

To propose a performance based framework for the case under study, we start by defining the limit states and the corresponding strain thresholds in the pipeline. The information provided by design codes (e.g. Eurocode 8, 2006) and guidelines (e.g. ALA, 2001; 2005) is usually provided in terms of strain thresholds and sometimes, of ovalization measures at the ultimate limit state. Longitudinal strain levels stated in Eurocode 8 corresponding to the ultimate limit states, are:

$$\varepsilon_{l,tu} = 0.03 \tag{6a}$$

$$\varepsilon_{l,cu} = \min(0.01, 0.2t/R_e) \tag{6b}$$

where; $\varepsilon_{l,tu}$ and $\varepsilon_{l,cu}$ are the tensile and compressive longitudinal ultimate strains; t is the pipe thickness; R_e is the external radius of the pipe cross-section.

Concerning the elastic strain limits, one may define the longitudinal yield strain couple ($\varepsilon_{l,ty}$ and $\varepsilon_{l,cy}$) as defined by $\varepsilon_{l,ty} = \left[\sigma_{l,ty} - \left(\sigma_l^p + \sigma_l^{\Delta T}\right)\right]/\mathrm{E}$ and $\varepsilon_{l,cy} = \left[\sigma_{l,cy} - \left(\sigma_l^p + \sigma_l^{\Delta T}\right)\right]/\mathrm{E}$ (Please refer to Equations 2, 3, and 4 for the calculations of σ_l^p, $\sigma_l^{\Delta T}$, and $\sigma_{l,ty}$ & $\sigma_{l,cy}$; respectively).

Let us define now LS1 and LS3 as the limit states corresponding to the no damage and to the ultimate states, respectively. We can, then, define LS1 as the first yield and LS3 for the ultimate state. In this paper, LS2, standing for the limited damage state, will be left only in terms of qualitative discussion; the engineer/analyst will define this limit according to the project under consideration. Once the maximum tensile and compressive longitudinal strains are tracked and output, the plot of maximum longitudinal strain versus the fault displacement can be plotted to provide the *capacity curve* of the fault-soil-structure interaction problem under consideration. See Figure 4 for an example of capacity curve from the considered numerical analysis.

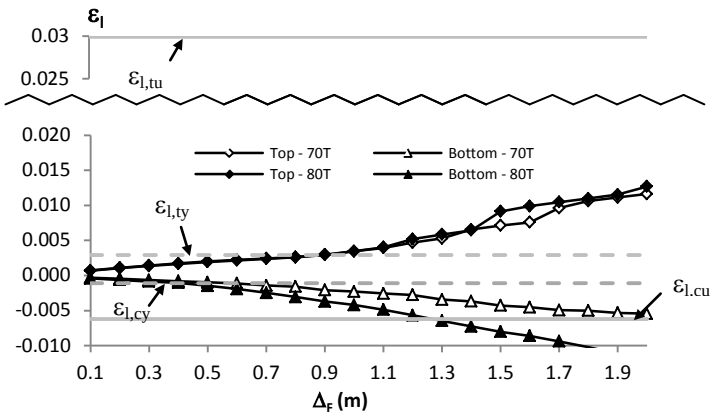

Limit State	Fault offset δ [m]	Definition
LS1	≅ 0.6 m	First yield in compression
LS3	>2.0 m	Ultimate compressive strain limit

Figure 4: *Left:* Capacity curves for *dip*=70° and 80°, *ΔT*=45°C, *p*=7.5 atm. *Right:* Corresponding limit state values for *dip*=70° and 80°, *ΔT*=45°C, *p*=7.5 atm.

Figure 4 shows the performance of the designed pipeline. For example, for *dip*=70°, *ΔT*=45°C, *p*=7.5 atm, the pipeline experiences the first yield (LS1) in compression at around fault offset of 0.6 m. Although ultimate limit state (LS3) has not been reached until Δ_F=2.0m for *dip*=70°, it could be seen that for *dip*=80°, the compressive strain is exceeded at 1.3 m. Since normal-fault crossing induces additional tensile strains to the pipeline, the outcome of reaching the ultimate state in terms of compression is neither trivial nor expected. This result is stemming from the initial compressive state of the pipeline due to increase in temperature of *ΔT*=45°C and relatively low horizontal elongation caused by the normal fault of *dip*=80°.

Conclusions

In this paper, we have illustrated the fundamental components for conducting accurate finite modeling of normal fault-soil-pipeline interaction problem. On a practical application, we also proposed a performance-based framework for interpreting the analysis results, by making use of EC8-based provisions. The problem of normal fault-soil-pipeline interaction has also been studied with analytical means; however it could not be included here due to space limitations. Interested readers are kindly referred to the upcoming journal article.

References

ALA. *Guidelines for the design of buried steel pipe*. American Lifeline Alliance, website: www.americanlifelinealliance.org, 2001.

ALA. *Seismic guidelines for water pipelines*. American Lifeline Alliance, website: www.americanlifelinealliance.org, 2005.

Bransby MF, Davies MCR, El Nahas A. Centrifuge modeling of normal fault-foundation interaction. *Bulletin of Earthquake Engineering* 2008; **6**(4): 585-605.

CEN, European Committee for Standardization. *Eurocode 8-Design of structures for earthquake resistance, Part 4: Silos, tanks and pipelines*. Final draft, 2006, preEn 1998-4.

Dassault Systèmes. *Abaqus 6.13*, Finite element code and the documentation, 2013.

Gaudin C. *Modélisation physique et numérique des écrans de soutènement: application a l'étude de l'effet d'une surcharge sur le sol soutenu*. PhD Thesis, Université de Nantes, 2002 (in French).

Karamitros DK, Bouckovalas GD, Kouretzis GP. Stress analysis of buried pipelines at strike-slip fault crossings. *Soil Dynamics and Earthquake Engineering* 2007; **27**: 200-211.

Karamitros DK, Bouckovalas GD, Kouretzis GP, Gkesouli V. An analytical method for strength verification of buried pipelines at normal fault crossings. *Soil Dynamics and Earthquake Engineering* 2011; **31**: 1452-1464.

Kennedy RP, Willianson RA, Chow AW Fault movement effects on buried oil pipeline. *Journal of Transportation Engineering* (ASCE) 1977; 103: 617-633.

Newmark NM, Hall WJ. Pipeline design to resist large fault displacements. *Proceedings of U.S. National Conference on Earthquake Engineering* 1975: 416-425; Ann Arbor, MI.

Paolucci R., Griffini S., Mariani S. Simplified modelling of continuous buried pipelines subject to earthquake fault rupture. *Earthquakes and Structures* 2010; **1**(3): 253-267.

Trifonov OV and Cherniy VP. A semi-analytical approach to a nonlinear stress-strain analysis of buried steel pipelines crossing active faults. *Soil Dynamics and Earthquake Engineering* 2010; **30**: 1298-1308.

Trifonov OV and Cherniy VP. Elastoplastic stress-strain analysis of buried steel pipelines subjected to fault displacements with account for service loads. *Soil Dynamics and Earthquake Engineering* 2012; **33**: 54-62.

Trifonov OV Numerical stress-strain analysis of buried steel pipelines crossing active strike-slip faults with an emphasis on Fault modeling aspects. *Journal of Pipeline Syst. Eng. Pract.* (ASCE) 2015; **6**.

Wang LRL and Yeh Y. A refined seismic analysis and design of bried pipeline for fault movement. *Earthquake Engineering and Structural Dynamics* 1985; **13**: 75-96.

Xie X, Symans MD, O'Rourke MJ, Abdoun TH, O'Rourke TD, Palmer MC, Stewart H. Numerical modeling of buried HDPE pipelines subjected to normal faulting: a case study. *Earthquake Spectra* 2013; **29**(2): 609-632.

Vazouras P, Karamanos SA, Dakoulas P. Buried steel pipelines crossing strike-slip faults, *Twenty-second (2012) International Offshore and Polar Engineering Conference* 2012: 365-372; Rhodes, Greece.